Supplementary file for Singh et al.

Materials and methods

Plasmid construction – Plasmids used in this study are listed in Table S1. Oligodeoxyribonucleotides used to make these plasmids or perform other experiments are listed in Table S2. To prepare YDpA-SUI3 and -SUI3-2, we subcloned the 1.8-kb *SUI3* or *SUI3-2* fragment of p2122 and p2192 (8) into pRS412 (*CEN ADE2*), respectively. To prepare YEpU-TIF5Δ20, the EcoRI-HindIII 2.3-kb fragment of YEpL-TIF5Δ20 (M. J. Murai and KA, unpublished material) was cloned into YEplac195.

For GST pull-down studies, pGEX-4G2ΔSHp, pGEX-4G2ΔSN and pGEX-4G2ΔN were constructed by transferring the NdeI-SalI eIF4G2-coding segments of pT7-4G2ΔSHp (7), pT7-4G2ΔSNr (H. Hui and KA, unpublished material) and pT7-4G2ΔN (7) to the same sites of pGEX-TIF5 (2). To generate pGEX-4G2ΔH, pGEX-4G2ΔNc, pGEX-4G2ΔN DNA digested with HindIII and NcoI was filled-in with klenow enzyme and self-ligated.

Other GST-eIF4G2 fusion constructs used in this study carry the B1 domain of streptococcal protein G (GB) as a solubility enhancement tag (14), in order to better express the recombinant eIF4G2 segment in bacteria. For this purpose, we produced a GST-GB1 fusion vector as follows. pGEX-TIF35 has multiple cloning sites (MCS) both 5` and 3` of the NdeI and PstI sites, respectively, used to clone *TIF35* ORF (4). Two BamHI sites in the MCS 5` of *TIF35* ORF were disrupted by digesting pGEX-TIF35 with BamHI followed by filling-in and self-ligation. The resulting plasmid pKA933 still encodes an in-frame GST-Tif35p fusion protein including the first Met codon of Tif35p

located in the unique NdeI site. pGEX-GB-Bm was constructed by subcloning the 0.2-kb NdeI-HindIII fragment of pGBfusion1 (14) into the same sites of pKA933. pGEX-GB-Bm has a unique BamHI site, an in-frame His_6-tag-coding region and a stop codon, EcoRI, SacI, SalI, HindIII and SphI sites for subcloning, after the GST-GB1-coding region. To create pGEX-GB-4G2ΔNr, the 1.2-kb NruI-SalI fragment of pGEX-GB-4G2ΔS-His was cloned into the BamHI-SalI site of pGEX-GB-Bm after the BamHI site of the latter was filled-in with klenow enzyme.

To make the *tif4632-7R* derivative of pGEX-GB-4G2ΔS, oligos GB-NdeI and 4G2-7R-R, or 4G2-Nr-F and 4G2-Bm-R were used for PCR using pGEX-GB-4G2ΔS or pAS2077 as template to amplify 0.3-kb or 1.3-kb fragments, respectively. Then oligos GB-NdeI and 4G2-Bm-R were used for PCR with both the 0.3-kb or 1.3-kb fragments as template to amplify a 1.6-kb fragment, followed by HindIII digestion. HindIII cleaves *TIF4632* ORF DNA at nt. 1986-1991. Thus, the NdeI-HindIII 0.7kb fragment encompassing GB-coding region, followed by the first ~640-bp of $eIF4G2_{439-914}$ coding region, was cloned into the same sites of pGEX-4G2ΔS (7), generating pGEX-GB-4G2ΔS-7R.

To make the pGEX-GB-4G2ΔSNr *7R* mutant derivative, pGEX-GB-4G2ΔS-7R was digested with NruI (which cuts at the 3` end of $eIF4G2_{439-513}$ coding region) and SalI (which cuts at the vector cloning site 3` of $eIF4G2_{439-914}$ coding region), and the larger NruI-SalI fragment of the reaction was self-ligated after filling-in with the klenow enzyme.

GST-SUI1-M4 was constructed by transferring the 0.7-kb NdeI-HindIII fragment of YCpL-SUI1-M4 into the same sites of pGEX-TIF35 (4).

For yeast expression studies, the *tif4632* mutant derivatives of pAS2077 (*HA-TIF4632 TRP1*) were generated as follows: For *tif4632-7R*, oligos 4G2-Nd-201 and 4G2-7R-R were used for PCR with pAS2077 as template to amplify a 0.9kb fragment. Then this fragment was cloned into pGEM T vector to generate Tvector-4G2-7R encoding nt. 601 – 1541 of eIF4G2 ORF with the 7R mutation. Then oligos 4G2-Nd-201 and 4G2-Nr-R, or 4G2-Nr-F and 4G2-Bm-R, were used for PCR using the Tvector-4G2-7R and pAS2077 as template to amplify 0.9-kb and 1.1-kb fragments, respectively. Oligos 4G2-Nd-201 and 4G2-Bm-R were used for PCR with both the 0.9kb and 1.1kb fragment as template to amplify a 2.0kb fragment. The NcoI-HindII 1.3kb fragment of this was cloned into the same sites of a plasmid created by cloning the NcoI-EcoRI 2.0kb fragment of pAS2077 encompassing the 3` two thirds of *TIF4632* ORF into pET15b. The NcoI-EcoRI 2.2kb fragment of the resulting plasmid was cloned into the same sites of pAS2077 to create YCpW-4G2-7R.

For *tif4632-ΔN*, the 0.75-kb NdeI-NcoI fragment of pAS2077 was replaced with double-stranded oligo made with HA-FW and HA-RV (Table S2), yielding YCpW-4G2-ΔN. For *tif4632-ΔX*, the 0.6-kb HindIII-XbaI fragment encompassing the aa. 653 – 846 of *tif4632* ORF was cloned into YEplac112 to add an EcoRI site 3' of the eIF4G2 deletion fragment. The 0.6-kb HindIII-EcoRI fragment of the resulting plasmid was cloned into the same site of pAS2077 to obtain YCpW-4G2-ΔX. This plasmid expresses HA-eIF4G2(1-846) fused C-terminally to a 13 aa.-long peptide (GSPGTELEFKIFF-stop) that is encoded by the vector sequence. In contrast, pGEX-GB-eIF4G2ΔSX (Table S2) encodes GST-GB1-eIF4G2(438-846) fused C-terminally to a decapeptide (VDSSGRIVTD-stop) that is encoded by the vector sequence.

References

1. **Asano, K., J. Clayton, A. Shalev, and A. G. Hinnebusch.** 2000. A multifactor complex of eukaryotic initiation factors eIF1, eIF2, eIF3, eIF5, and initiator $tRNA^{Met}$ is an important translation initiation intermediate in vivo. Genes Dev **14:**2534-2546.
2. **Asano, K., and A. G. Hinnebusch.** 2001. Protein interactions important in eukaryotic translation initiation, p. 179-198. *In* P. N. MacDonald (ed.), Two Hybrid Systems, Methods and Protocols, vol. 177. Humana Press, Inc., Totowa, NJ.
3. **Asano, K., P. Lon, T. Krishnamoorthy, G. D. Pavitt, G. E., E. M. Hannig, J. Nika, T. F. Donahue, H.-K. Huang, and A. G. Hinnebusch.** 2002. Analysis and Reconstitution of Translation Initiation In Vitro. Methods in Enzymology **351:**221-247.
4. **Asano, K., L. Phan, J. Anderson, and A. G. Hinnebusch.** 1998. Complex formation by all five homologues of mammalian translation initiation factor 3 subunits from yeast *Saccharomyces cerevisiae*. J Biol Chem **273:**18573-18585.
5. **Asano, K., A. Shalev, L. Phan, K. Nielsen, J. Clayton, L. Valasek, T. F. Donahue, and A. G. Hinnebusch.** 2001. Multiple roles for the carboxyl terminal domain of eIF5 in translation initiation complex assembly and GTPase activation. EMBO Journal **20:**2326-2337.
6. **Asano, K., H.-P. Vornlocher, N. J. Richter-Cook, W. C. Merrick, A. G. Hinnebusch, and J. W. B. Hershey.** 1997. Structure of cDNAs encoding human eukaryotic initiation factor 3 subunits: possible roles in RNA binding and macromolecular assembly. J Biol Chem **272:**27042-27052.
7. **He, H., T. von der Haar, R. C. Singh, M. Ii, B. Li, A. G. Hinnebusch, J. E. G. McCarthy, and K. Asano.** 2003. The yeast eIF4G HEAT domain interacts with eIF1 and eIF5 and is involved in stringent AUG selection. Molecular and Cellular Biology **23:**5431-5445.
8. **Huang, H., H. Yoon, E. M. Hannig, and T. F. Donahue.** 1997. GTP hydrolysis controls stringent selection of the AUG start codon during translation initiation in *Saccharomyces cerevisiae*. Genes Dev **11:**2396-2413.
9. **Neff, C. L., and A. B. Sachs.** 1999. Eukaryotic translation initiation factors eIF4G and eIF4A from *Saccharomyces cerevisiae* physically and functionally interact. Molecular and Cellular Biology **19:**5557-5564.
10. **Reibarkh, M., Y. Yamamoto, C. R. Singh, F. d. Rio, A. Fahmy, B. Lee, R. E. Luna, M. Ii, G. Wagner, and K. Asano.** 2008. Eukaryotic initiation factor (eIF) 1 carries two distinct eIF5-binding faces important for multifactor assembly and AUG selection J Biol Chem **283:**1094-1103.
11. **Singh, C. R., H. Hui, M. Ii, Y. Yamamoto, and K. Asano.** 2004. Efficient incorporation of eIF1 into the multifactor complex is critical for formation of

functional ribosomal preinitiation complexes in vivo. Journal of Biological Chemistry **279:**31910-31920.
12. **Tarun, S. Z., and A. B. Sachs.** 1997. Binding of eukaryotic translation initiation factor 4E (eIF4E) to eIF4G represses translation of uncapped mRNA. Molecular and Cellular Biology **17:**6876-6886.
13. **Watanabe, R., M. J. Murai, C. R. Singh, S. Fox, M. Ii, and K. Asano.** 2010. The eIF4G HEAT domain promotes translation re-initiation in yeast both dependent on and independent of eIF4A mRNA helicase. J Biol Chem **285:**21922-21933.
14. **Zhou, P., A. A. Lugovskoy, and G. Wagner.** 2001. A Solubility-Enhancement Tag (SET) for NMR Studies of Poorly Behaving Proteins. J. Biomol. NMR **20:**11-14.

Legends to supplemental figures

Fig. S1. Effect of eIF1 mutations on binding to GST-eIF4G2-A. (A) The line on top indicates the amino acid sequence of yeast eIF1 (y eIF1), with red and blue boxes denoting α helices and β sheets, respectively. Shown below are the blocks of sequences indicating mutations (*M1-M5*; altered amino acids are shown in red) used in this figure. eIF1-NTT is highlighted in green. Boxed with light blue are the FLAG-epitope sequences introduced. (B) Space-filled model of yeast eIF1, indicating surface charge distribution (blue, positive; red, negative). Circled are the location of KH and KR areas of the globular domain and acidic patches in the NTT. (C) 5 μg of GST alone (GST, lanes 2), -eIF3c$_{1\text{-}156}$ (3c-N, lane 3), or –eIF4G2$_{439\text{-}914}$ (4G2-A, lane 4) was allowed to bind ^{35}S-eIF1 or its derivatives carrying *M1-M4* that had been expressed in the TnT system (Promega) from appropriate plasmids (10) (second and fifth gels), or ~10 μg of recombinant eIF1 or eIF1-*M5* (sixth and seventh gels), expressed in BL21(DE3) carrying pET-SUI1 or pET-SUI1-M5 (10), respectively, as described (11). The complex was isolated and analyzed by SDS-PAGE followed by Coommssie staining (top gels), STORM phosphorimager (Molecular Dynamics) (second and fifth gels), or

immunoblotting with anti-eIF1 antibodies (sixth and seventh gels). Lanes 1, 10 or 2 % input amounts of ^{35}S-eIF1 or bacterially expressed recombinant eIF1 (r-eIF1), respectively. Effect of each mutation on eIF3c or eIF4G2 binding was shown below each gel by % compared to the relative fraction of wild-type eIF1 bound to each GST fusion protein. Note that a minor fraction of eIF1-*M5* binds to GST alone in lane 2, suggesting that a part of expressed eIF1-*M5* binds non-specifically to GST or resin. Because eIF1-*M5* bound to GST-eIF4G2-A to this level, *M5* was judged to abolish interaction with eIF4G2 ("-" under the gel). Lanes 1-3 are adapted from (10).

Fig. S2. A minimal binding segment of eIF4G2 for RNA and Pab1p. (A) Northwestern blot experiments conducted on the recombinant eIF4G2 constructs together with GST alone as negative control. Proteins indicated across the top are immobilized on a nitrocellulose membrane after SDS-PAGE and incubated with ^{32}P-β-globin mRNA (~20,000 cpm) (6). After washing, the autoradiography was taken with a phosphorimager (bottom panel). The proteins on the membrane were later visualized by Ponceau staining (top panel). Arrowheads on the top panel indicate the expected location of the full-length products; the same arrowheads on the bottom panels show the RNA bound to the full-length products. The asterisk indicated the RNA-binding activity of *E. coli* proteins that contaminated from bacterial lysates (6) in some of the fractions used here. eIF4G2 proteins used here are defined in Fig 1A. (B) GST fusion to different N-terminal segments of eIF4G2 (top panel, labeled as in Fig. 1A) was subjected to binary interaction assay with ^{35}S-Pab1p (bottom panel) expressed in rabbit reticulocyte and analyzed as in Fig. 1B. Lane 1 indicates the 20% input amount of ^{35}S-Pab1p used in this assay. The

percentage of ^{35}S-Pab1p bound to each of GST fusion protein is shown below the autoradiography.

Fig. S3. Statistical analysis of ^{32}P-*MFA2* mRNA binding to 40S subunit in yeast cell extracts. Graphs indicate the % of ^{32}P-*MFA2* mRNA bound to 40S subunits in indicated mutant cell extracts, compared to the amount of ^{32}P-*MFA2* mRNA bound to 40S subunits in wild-type cell extracts, with *p* values for the designated differences. Panels A and B, analyses of experiments shown in Fig. 2C and 3C, respectively, and other independent experiments. The 40S-bound ^{32}P-mRNA peak appears on the shoulder of the major, free ^{32}P-mRNA peak. Therefore, the amount of ^{32}P-mRNA bound to the 40S subunit was obtained by subtracting the (hypothetical) background values from the raw scintillation counting data and compared to that from the control experiment using the wild-type extracts. **no peak*: When experiments were done with extracts prepared from *tif4632-ΔN* in (A), column 4, there was no peak observed in fractions corresponding to the free 40S subunit ("no peak" or value of zero).

Fig. S4. Effect of eIF1 and eIF5-C addition on mRNA binding to the 43S complex in cell extracts prepared from *tif4632-7R*. Cell-free translation extracts from the mutants and wild type were prepared and used to set up a reaction (50 μl) with ^{32}P-labeled poly(A)-tailed *MFA2* mRNA (3). The reaction mixture with or without addition of indicated proteins (20 μg) was fractionated by sucrose gradient velocity sedimentation, and gradient samples were analyzed by scintillation counting. ^{32}P counts in relevant fractions are shown with an arrow indicating the fraction containing free 40S subunit.

Fig. S5. Experimental design to test the effect of eIF5 addition on ^{32}P-β-globin mRNA binding by GST-eIF4G2 fusions. (A) Purified GST-eIF4G2 fusion proteins (1-3

μg) used in Fig. 4 were incubated with ^{32}P-β-globin mRNA (~20,000 cpm), precipitated, and the percentage of the RNA co-precipitated was determined by scintillation counting,. Bars indicate standard errors. (B) Experimental design to measure the effect of eIF5 on mRNA binding by eIF4G2 constructs. Difference in values of GST pull down in (A) results from different amounts of GST fusion proteins bound to the glutathione resin. To ensure accurate comparison, we first bound GST fusion proteins to ~10 μl bed volume of glutathione resin, split the protein-bound resin to half in two tubes, then added eIF5 in one tube, as depicted in (B). The other tube was left blank as control. Then ^{32}P-β-globin mRNA was added to each tube and the mRNA binding was assayed as described above.

Table S1. Plasmids used in this study

Plasmid	Description	Source
Plasmids used for yeast genetics		
pAS2077	Single-copy *HA-TIF4632 TRP1* plasmid	(12)
YCpW-4G2-7R	pAS2077 carrying *tif4632-7R*	This study
YCpW-4G2-ΔX	pAS2077 carrying *tif4632-ΔX (aa. 1-846) lacking C-terminal 68 amino acids*	This study
YCpW-4G2-ΔA	pAS2077 carrying *tif4632-ΔA (aa. 1-814) lacking C-terminal 100 amino acids*	This study
YCpW-4G2-ΔN	pAS2077 carrying *tif4632-ΔN (aa. 238-914). lacking N-terminal 237 amino acids.*	This study
YDpU-SUI3	Low-copy *SUI3 URA3* plasmid	(13)
YDpU-SUI3-2	Low-copy *SUI3-2 URA3* plasmid	(13)
YEpU-SUI1	High-copy *SUI1 URA3* plasmid	(7)
pAS3434	High-copy *TIF2 URA3* plasmid	(9)
YEpU-TIF5	High-copy *TIF5 URA3* plasmid	(7)
YEpU-TIF5Δ20	High-copy *tif5Δ20-FL URA3* plasmid	This study
Plasmids used to express GST-fusion proteins		
pGEX-GB-4G2ΔS	GST-GB-eIF4G2$_{439-914}$ fusion plasmid	(13)
pGEX-4G2ΔSHp	GST-eIF4G2$_{439-577}$ fusion plasmid	This study
pGEX-4G2ΔSNr	GST-eIF4G2$_{439-513}$ fusion plasmid	This study
pGEX-4G2ΔN	GST-eIF4G2$_{1-513}$ fusion plasmid	This study
pGEX-4G2ΔH	GST-eIF4G2$_{1-172}$ fusion plasmid	This study
pGEX-4G2ΔNc	GST-eIF4G2$_{1-239}$ fusion plasmid	This study
pGEX-4G2ΔAf	GST-eIF4G2$_{816-914}$ fusion plasmid	(13)
pGEX-GB-Bm	GST-GB1 fusion vector with a BamHI site	This study
pGEX-GB-4G2ΔNr	GST-GB-eIF4G2$_{514-914}$ fusion plasmid	This study
pGEX-GB-4G2ΔSX	GST-GB-eIF4G2$_{439-846}$ fusion plasmid	(13)
pGEX-GB-4G2ΔS-7R	pGEX-GB-4G2ΔS carrying *tif4632-7R*	This study
pGEX-GB-4G2ΔSNr	GST-GB-eIF4G2$_{439-513}$ fusion plasmid	(13)
pGEX-GB-4G2ΔSNr-7R	pGEX-GB-4G2ΔSNr carrying *tif4632-7R*	This study
pGEX-GB-4G2ΔSNr-8*	pGEX-GB-4G2ΔSNr carrying *tif4632-8**	(13)

pGEX-SUI1*	GST-eIF1 fusion plasmid	(11)
pGEX-SUI1-M4	pGEX-SUI1 carrying *sui1-M4*	This study
pGEX-SUI1-M5	pGEX-SUI1 carrying *sui1-M5*	(10)
pGEX-SUI3ΔS	GST-eIF2$\beta_{1\text{-}140}$ fusion plasmid	(11)
Plasmids used to express recombinant eIF-binding partners		
pT7-4G2ΔS	eIF4G2$_{439\text{-}914}$ under T7 *p* cloned in pT7-7	(5)
pT7-SUI1	eIF1 cloned under T7 *p* in pT7-7	(1)
pET-TIF1	eIF4A1 cloned under T7 *p* in pET28c	J. McCarthy
pHis-TIF5-B6	eIF5-C (eIF5$_{241\text{-}405}$) cloned under T7 in pET15b	(1)
pT7-PAB1	Pab1p cloned under T7 *p* in pT7-7	C. R. Singh
pET-His-SUI1	His$_6$-eIF1 cloned under T7 *p* in pET15b	(10)

Table S2. Oligodeoxyribonucleotides used in this study

Name	Sequence (5` to 3`), restriction sites underlined	Description
GB-Nd-F	CCC ATA TGC AGT ACA AAC TGA TCC TG	GB1 ORF nt. 1-21
4G2-Bm-F	GGC CGG ATC CCC TGA TCC TGC GTG GGT TG	*TIF4632* ORF nt 1315 to 1333
4G2-Bm-R	GGC CGG ATC CAT CAC TGT CCC CAT CGT TAT TC	*TIF4632* ORF nt. 2721 to 2742
4G2-7R-R	CCC TCG CGA TCT TTT CTG GAG GTA TAT CCC TGA TTA GAC TGC TGG TCG TCA CCC ATC TGC TTT GAC TGC TGT TTC GAT GAA ACC TGT GAA CTG GAA GTA TG	*TIF4632* ORF nt. 1444 to 1541 with the 7 R-to-Q mutation
4G2-Nr-F	TAT ACC TCC AGA AAA GAT CG	*TIF4632* ORF nt. 1519 to 1538
4G2-Nr-R	TTT TTC GCG ATC TTT TCT GG	*TIF4632* ORF nt. 1526 to 1545
4G2-Nd-201	GGG CAT ATG GCT AAT GAA GCA GTT AAA GAT	*TIF4632* ORF nt. 601 to 621
HA-FW	TAT GTA CCC ATA CGA CGT CCC AGA CTA CGC	HA-epitope, forward
HA-RV	CAT G GCG TAG TCT GGG ACG TCG TAT GGG TAC A	HA-epitope, reverse

Table S3. *S. cerevisiae tif4632* strains used in this study

tif4632 allele	**Amino acid change**	**Mutated domain**	**Interaction impaired**	*GCN2*$^{+}$ strains[a]	*his4*$^{AUU/UU\ G}$ strains[b]
1 *WT*	Wild-type			YAS1955	KAY220
2 *tif4632-7R*	R487Q R492Q R493Q R496Q R501Q R502Q R505Q	RS 1	eIF1, eIF5, RNA	KAY874, KAY901	KAY862
5 *tif4632-8**	R473I K491R R501S	RS 1	none found	KAY872	N. E.
6 *tif4632-ΔX*	Δ *(847-914).*	RS2	RNA	KAY873	KAY861
7 *tif4632-ΔN*	Δ(1-237)	RNA1, PABP-BD[c]	Pab1p, RNA	KAY856	KAY864

[a]Derivatives of YAS1955 (MATa *ade2-1 his3-11,15 leu2-3, ura3-1 trp1-1 pep4::HIS3 tif4631::LEU2 tif4632::ura3* p[*HA-TIF4632 TRP1*]) carrying indicated mutations (7, 12).

[b]Derivatives of KAY220 (MATa *ade2-1 his3-11,15 his4-303*$^{AUU/UUG}$ *leu2-3, ura3-1 trp1-1 pep4::HIS3 tif4631::LEU2 tif4632::ura3* p[*HA-TIF4632 TRP1*]) carrying indicated mutations. N. E., not employed in this study.

[c]HEAT domain made of five α-helical HEAT repeats (aa. 557 – 812 of 914 aa.-long eIF4G2).

Singh et al. Fig. S1

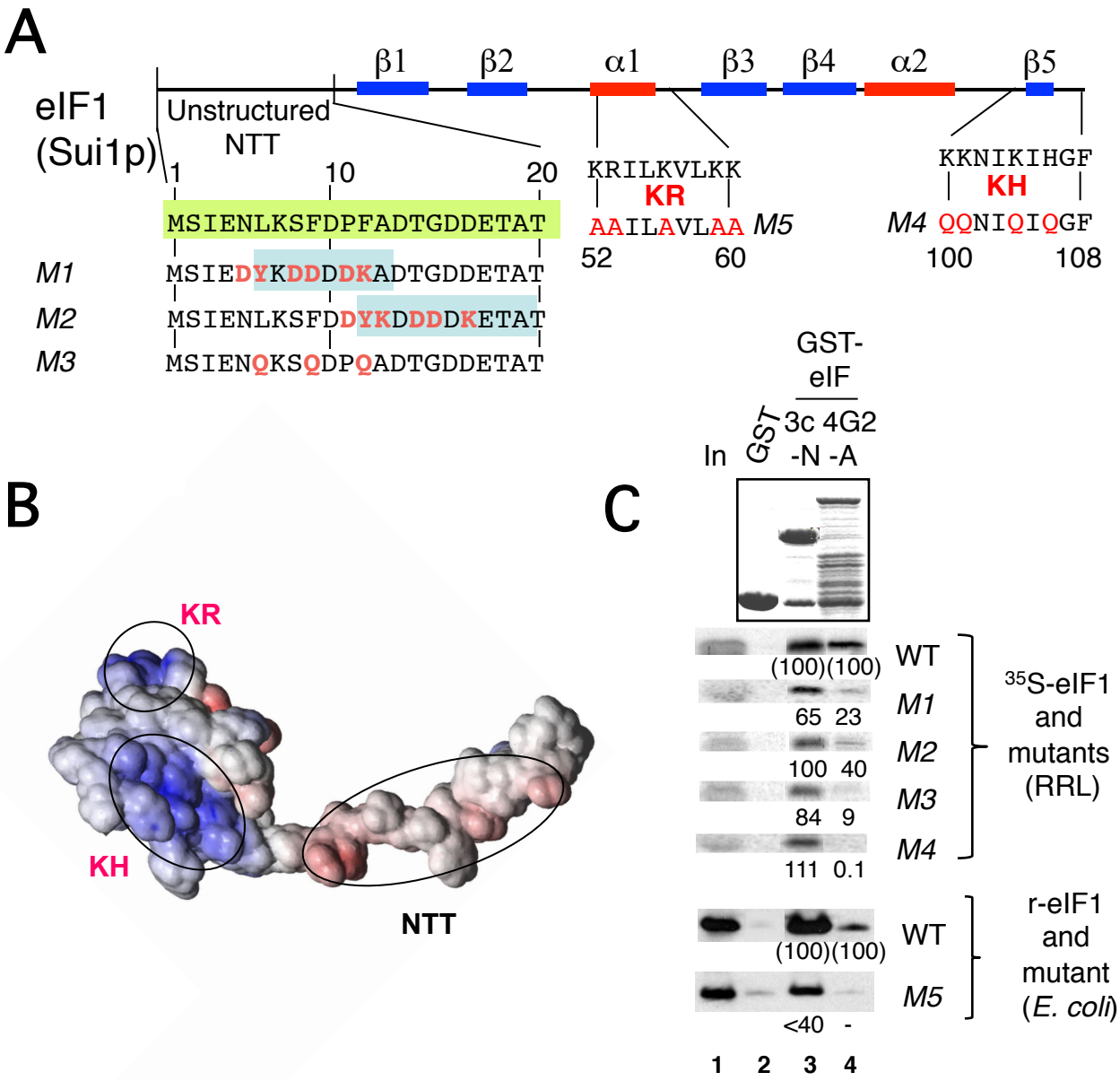

Singh Fig. S2

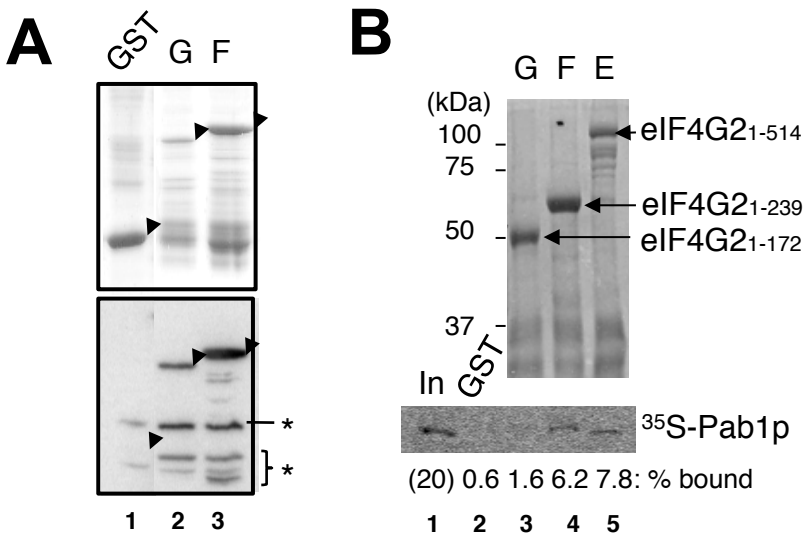
A
GST
G F
*
*
1 2 3
B
G F E
(kDa)
100
75
50
37
eIF4G2 1-514
eIF4G2 1-239
eIF4G2 1-172
In GST
35S-Pab1p
(20) 0.6 1.6 6.2 7.8: % bound
1 2 3 4 5

Singh Fig. S3

A

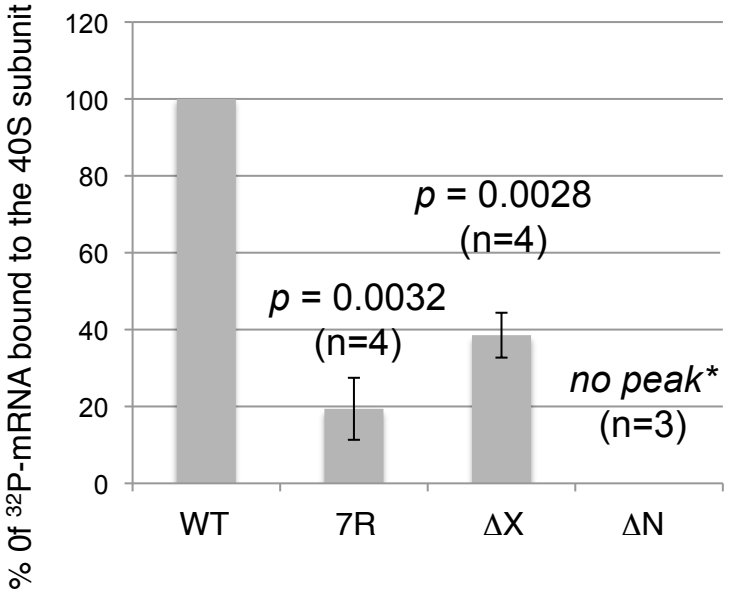

B

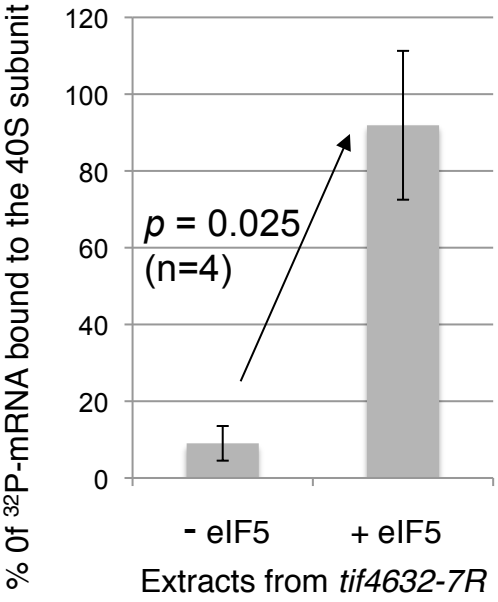

Singh Fig. S4

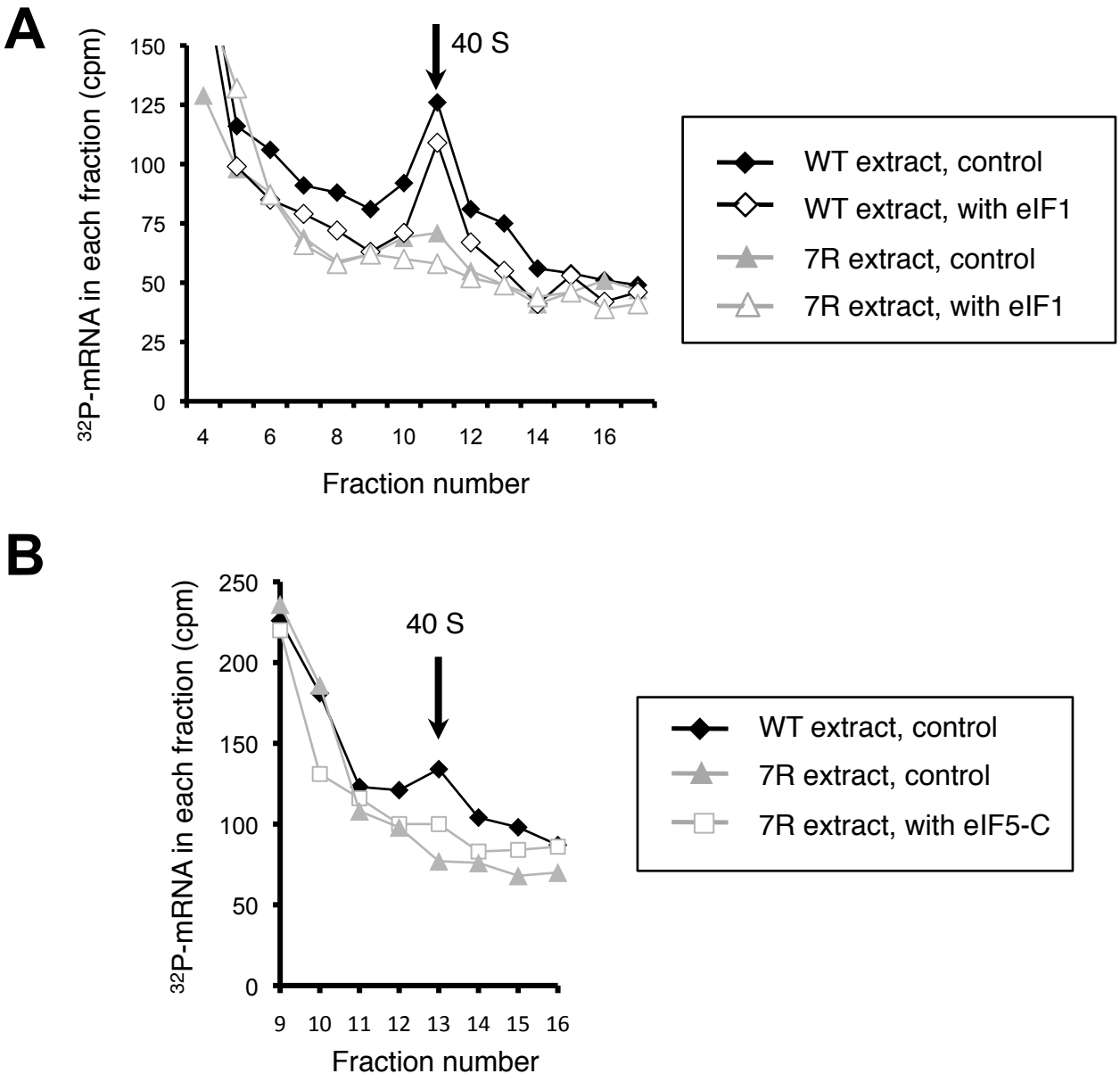
A
40 S
150
125
100
75
50
25
0
4
6
8
10
12
14
16
32P-mRNA in each fraction (cpm)
Fraction number
WT extract, control
WT extract, with eIF1
7R extract, control
7R extract, with eIF1
B
40 S
250
200
150
100
50
0
9
10
11
12
13
14
15
16
32P-mRNA in each fraction (cpm)
Fraction number
WT extract, control
7R extract, control
7R extract, with eIF5-C

Singh Fig. S5

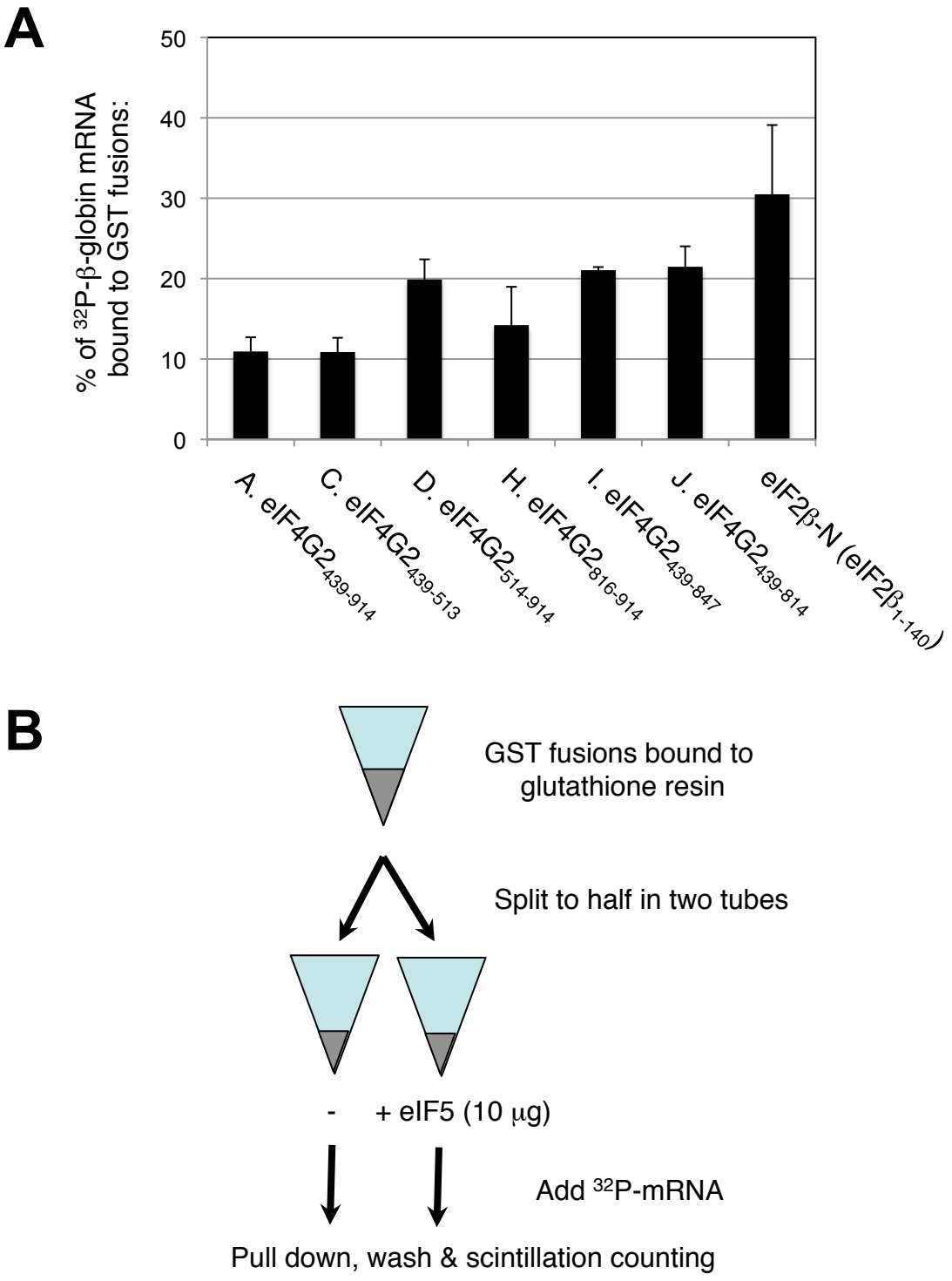
A
% of 32P-β-globin mRNA bound to GST fusions:
50
40
30
20
10
0
A. eIF4G2439-914
C. eIF4G2439-513
D. eIF4G2514-914
H. eIF4G2816-914
I. eIF4G2439-847
J. eIF4G2439-814
eIF2β-N (eIF2β1-140)
B
GST fusions bound to glutathione resin
Split to half in two tubes
- + eIF5 (10 μg)
Add 32P-mRNA
Pull down, wash & scintillation counting